Front. Phys., 2014, 9(4): 483–489
DOI 10.1007/s11467-014-0414-4

RESEARCH ARTICLE

# LDA+$U$ calculation of structural and thermodynamic properties of $Ce_2O_3$

**Bo Zhu**[1], **Yan Cheng**[1,2,*], **Zhen-Wei Niu**[1], **Meng Zhou**[1], **Min Gong**[1,2,†]

[1] *College of Physical Science and Technology, Sichuan University, Chengdu 610064, China*

[2] *Key Laboratory of High Energy Density Physics and Technology of Ministry of Education, Sichuan University, Chengdu 610064, China*

*Corresponding authors. E-mail: *ycheng@scu.edu.cn, †mgong@scu.edu.cn*

*Received May 21, 2013; accepted September 26, 2013*

We investigated the structure and thermodynamic properties of the hexagonal $Ce_2O_3$ by using LDA+$U$ scheme in the frame of density functional theory (DFT), together with the quasi-harmonic Debye model. The obtained lattice constants, bulk modulus, and the insulating gap agree well with the available experimental data. We successfully yielded the temperature dependence of bulk modulus, volume, thermal expansion coefficient, Debye temperature, specific heat as well as the entropy at different $U$ values. It is found that the introduction of the $U$ value cannot only correct the calculation of the structure but also improve the accurate description of the thermodynamic properties of $Ce_2O_3$. When $U = 6$ eV the calculated volume (538 Bohr$^3$) at 300 K agrees well with the experimental value (536 Bohr$^3$). The calculated entropy curve becomes more and more close to the experimental curve with the increasing $U$ value.

**Keywords** density functional theory, thermodynamic properties, quasi-harmonic Debye model, $Ce_2O_3$

**PACS numbers** 71.15.Mb, 61.50.Ks



## 1 Introduction

Cerium oxides, as important materials with remarkable properties, are applied in a number of technological products, such as in industrial catalysis [1] and scintillator material [2]. Since it is not only a high-yield fission product but also a substitute of plutonium in nuclear fuels research, the thermodynamic properties of cerium oxides are extensively studied in nuclear technology [3]. Exact calculations of the structure and thermodynamic properties of cerium oxides in extreme conditions are primary of interest in their future applications.

As a high-yield fission product, the thermodynamic properties of the cerium oxides have been formed a series of interesting studies in theories and experiments. In 1969, Justice *et al.* [4] reported the low temperature thermal capacities of $Ce_2O_3$ from 5 K to 350 K and obtained the heat capacity $C_p$ at 298.15 K. In the experiment of Huntelaar *et al.* [5], the thermodynamic properties of $Ce_2O_3$ measured in the temperature range from 3 K to 420 K and from 470 K to 883 K and extrapolating to 1500 K. Developing reliable theoretical model of such properties is a significant help, especially for the direction of experiments at high temperatures.

The ground state structure of a material is directly linked to the structure and thermodynamic properties of the material at high temperatures. However, the standard LDA (local density approximation) and GGA (generalized gradient approximation) approaches have a major deficiency, i.e., the delocalization error, which can even lead to incorrect metallic ground state for $Ce_2O_3$ [6–8]. From recent calculations [8–12], LDA+$U$ method, in which a Hubbard $U$ term is added to LDA, is proved to be a good method to describe the strongly correlated systems that contain $4f$ states, like $Ce_2O_3$.

Recently, we have investigated the pressure dependences of elastic properties of $Ce_2O_3$ under pressure [13]. We here perform a systematic study of the thermodynamic properties of $Ce_2O_3$ within local density approximation with Hubbard corrections (LDA+$U$ approximation) through the Cambridge Serial Total Energy Package (CASTEP) program [14, 15], and apply the quasi-harmonic Debye model to investigate the ther-

modynamic properties of $Ce_2O_3$ under high pressure and high temperature with different $U$ values [16, 17].

This paper is organized as follows: the details of the methods used are described in Section 2. The results and some discussion of the crystal parameters, elastic constants, bulk and shear moduli, Debye temperature, specific heat and entropy are presented in Section 3. A conclusion of our main findings is given in Section 4.

## 2 Theoretical method and computation details

### 2.1 Total energy electronic structure calculations

In our electronic structure calculations, we employ the on-the-fly (OTF) pseudopotential for the interactions of the electrons with the ion cores, together with the local density approximation (LDA) proposed by Vosko *et al.* [18] for the exchange-correlation potential. The LDA has been used in the LDA+$U$ variant, in which the orbital-dependent LDA+$U$ functional form is given as

$$E_{\mathrm{LDA}+U} = E_{\mathrm{LDA}} + \frac{U-J}{2}\sum_{\sigma}[\mathrm{Tr}\rho^{\sigma} - \mathrm{Tr}(\rho^{\sigma}\rho^{\sigma})] \quad (1)$$

where $\rho^{\sigma}$ is the density matrix of the $f$ states, $U$ is the Coulomb energy, and $J$ is the exchange energy. In the approach, the Coulomb parameter $U$ and exchange parameter $J$ do not enter separately, but combine into a single meaningful parameter $U$ ($U_{\mathrm{eff}} = U - J$). A detailed description of this functional form can be found in Refs. [19, 20].

The electronic wave functions are expanded in a plane wave basis set with an energy cut-off of 620 eV. The atomic levels $4f^15s^25p^65d^16s^2$ for Ce atom and $2s^22p^4$ for O atom are treated as valence electron states. For the Brillouin-zone sampling, we use the 4×4×2 Monkhorst–Pack mesh [21]. The self-consistent convergence of the total energy is $1.0\times10^{-6}$ eV/Atom, the maximum ionic Hellmann–Feynman force within 0.01 eV/Å, the maximum ionic displacement within $1.0\times10^{-4}$ Å, and the maximum stress within 0.02 GPa. These parameters are carefully tested, and sufficient to lead to a well-converged total energy.

### 2.2 Thermodynamic properties

The quasi-harmonic Debye model [16, 17], in which the phononic and anharmonic effects are considered, has been applied successfully to investigate the thermodynamic properties of several materials [22–28]. We here apply it to investigate the thermodynamic properties of $Ce_2O_3$. In this quasi-harmonic Debye model, the non-equilibrium Gibbs function $G^*(V;P;T)$ can be written as

$$G^*(V;P;T) = E(V) + PV + A_{\mathrm{vib}}(T, \Theta_{\mathrm{D}}(V)) \quad (2)$$

where $E(V)$ is the total energy per formula unit, $PV$ corresponds to the constant hydrostatic pressure condition, $\Theta_{\mathrm{D}}(V)$ is the Debye temperature, and the vibrational Helmholtz free energy $A_{\mathrm{vib}}$ can be written as

$$A_{\mathrm{vib}}(\Theta_{\mathrm{D}};T) = nkT[\frac{9}{8}\frac{\Theta_{\mathrm{D}}}{T} + 3\ln(1-\mathrm{e}^{-\Theta_{\mathrm{D}}/T}) - D(\Theta_{\mathrm{D}}/T)] \quad (3)$$

where $D(\Theta_{\mathrm{D}}/T)$ represents the Debye integral, $n$ is the number of atoms per formula unit. For an isotropic solid, the Debye temperature $\Theta_{\mathrm{D}}$ is expressed as

$$\Theta_{\mathrm{D}} = \frac{\hbar}{k}[6\pi^2V^{1/2}n]^{1/3}f(\sigma)\sqrt{\frac{B_S}{M}} \quad (4)$$

where $M$ is the molecular mass, $B_S$ is the adiabatic bulk modulus, which is approximated by the static compressibility

$$B_S \cong B = V\left\{\frac{\mathrm{d}^2E(V)}{\mathrm{d}V^2}\right\} \quad (5)$$

$f(\sigma)$ is given by Refs. [16, 17], the Poisson $\sigma$ is taken as 0.3. Finally, the Gibbs function is minimized and the thermal equation of state is calculated. The non-equilibrium Gibbs function $G^*(V;P,T)$ as a function of $(V;P,T)$ can be minimized with respect to volume $V$

$$\left(\frac{\partial G^*(V;P,T)}{\partial V}\right)_{P,T} = 0 \quad (6)$$

By solving Eq. (6), one can get the isothermal bulk modulus $B_T$, heat capacity $C_V$, thermal expansion coefficient $\alpha$, the Grüneisen parameter $\gamma$, and the heat capacity $C_P$.

## 3 Results and discussion

### 3.1 Structural properties of $Ce_2O_3$

At ambient conditions, $Ce_2O_3$ is one of the strongly correlated insulating systems of the hexagonal sesquioxide (with point group $P\bar{3}m1$) with lattice parameters $a = 3.891$ Å and $c = 6.059$ Å [29]. We illustrate the unit cell crystal structure of the hexagonal $Ce_2O_3$ in Fig. 1. It is known that, for many strongly correlated insulating systems, the conventional density functional theory (DFT) calculations with LDA and GGA methods usually have the delocalization error. To solve this problem, one needs to apply some reasonable corrections for the

conventional DFT calculations, such as, hybrid density functional (HSE) [30, 31], LDA+$U$ [19, 20], and so on. By using the HSE, Hay *et al.* [30] obtained a correct description of the insulating nature of $Ce_2O_3$, but it is not a very good picture for the geometric and electronic structures [30]. We here used the LDA+$U$ to further investigate the structure of the hexagonal $Ce_2O_3$.

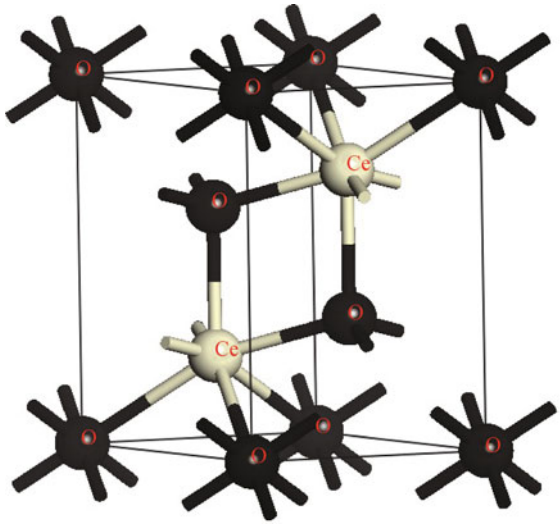


**Fig. 1** The conventional unit cell of the hexagonal structure $Ce_2O_3$. Black and grey balls represent O and Ce atoms, respectively.

In the equilibrium geometry calculations, we performed the following procedures: first, for a fixed axial ratio $c/a$, we took a series of different values of lattice parameters $a$ and $c$ to calculate the total energies $E$ and the corresponding primitive cell volumes $V$, and then obtained the lowest energy $E_{\min}$ for the given ratio $c/a$. This procedure was repeated over a wide range of $c/a$. Finally, by fitting our $E_{\min} - V$ data to the third-order Birch–Murnaghan equation of state (EOS) [32]

$$P(V) = \frac{3B_0}{2}\left[\left(\frac{V_0}{V}\right)^{\frac{7}{3}} - \left(\frac{V_0}{V}\right)^{\frac{5}{3}}\right] \cdot \left\{1 + \frac{3}{4}(B_0' - 4)\left[\left(\frac{V_0}{V}\right)^{\frac{2}{3}} - 1\right]\right\} \quad (7)$$

where $V_0$ is the equilibrium cell volume of $Ce_2O_3$ at 0 GPa and 0 K, and $V$ is the unit cell volume corresponding to the applied pressure $P$ at 0 K, we obtained the equilibrium lattice parameters $a, c$, $c/a$, the bulk modulus $B_0$ and its pressure derivative $B_0'$ of $Ce_2O_3$ when $U$ equals to 0, 2, 4, and 6 eV. All these results are listed in Table 1, together with the experimental data. It is found that the lattice parameters of $Ce_2O_3$ are sensitive to $U$. The lattice constants $a$ and $c$ are close to the experimental values (3.89 Å and 6.06 Å) [29] with the increasing $U$ value. The bulk modulus $B_0$ consistently decreases while its pressure derivative $B_0'$ increases upon the increasing $U$ value. According to the results of Loschen *et al.* [10], these results are due to the higher $U$ values leading to lower bonding/cohesive energies. Apparently, the $U$ values also affect the structure and related properties of $Ce_2O_3$ at high temperatures. However, as the $U$ value increases, the insulating gap is far away from the experimental value (2.4 eV) [33]. By comparing these results with each other, we note that the LDA+$U$ method with $U = 6$ eV seems to be more suitable for investigating the structural properties of $Ce_2O_3$. Using the LDA+$U$ method with $U = 6$ eV, we obtained the lattice parameters $a = 3.877$ Å and $c/a = 1.554$, as well as the insulating gap $E_{\text{gap}} = 2.72$ eV, which are consistent with the experimental results ($a = 3.891$ Å and $c/a = 1.557$ [29], $E_{\text{gap}} = 2.4$ eV [33]). In the following, we will mainly investigate the effect of $U$ value on the thermodynamic properties of $Ce_2O_3$ by using the LDA+$U$ method.

**Table 1** The lattice parameters, bulk modulus $B_0$ and its pressure derivative $B_0'$, and the insulating gap of $Ce_2O_3$ according to the calculations from LDA+$U$ with different $U$ values and experimental data.

| $U$ /eV | $a$ /Å | $c$ /Å | $B_0$ /GPa | $B_0\prime$ /GPa | Insulating gap /eV |
|---|---|---|---|---|---|
| 0 | 3.774 | 5.827 | 160.7 | 4.51 | 0 |
| 2 | 3.848 | 5.945 | 144.4 | 4.55 | 1.41 |
| 4 | 3.863 | 5.992 | 142.2 | 4.6 | 2.12 |
| 6 | 3.877 | 6.025 | 135.3 | 4.96 | 2.72 |
| Exp. [29, 33] | 3.89 | 6.06 | 111 | | 2.4 |

### 3.2 Thermodynamic properties

We now employ the calculated $E - V$ data of $Ce_2O_3$ obtained from LDA+$U$ to investigate the dependence of bulk modulus $B$ on temperature $T$ by using quasi-harmonic Debye model [16, 17]. In Fig. 2, we present the relationship of the bulk modulus of $Ce_2O_3$ as a function of temperature $T$ up to 1800 K when $U$ equals 0, 2, 4, and 6 eV, respectively. The calculated zero pressure bulk modulus $B_0$ from Eq. (7) is 138.4 GPa at 0 K and $U = 6$ eV, which is in agreement with the result obtained by Loschen *et al.* [10] ($B_0 = 144.7$ GPa) and Andersson *et al.* [11] ($B_0 = 130$ GPa). From Fig. 2, it can be found that $U$ value has little effect on $B_0$ when $U$ is lager than 4. The curves seem not smooth at high temperature region. The reason is that the rare earth elements form a sesquioxide, and three types designated as A, B, and C are commonly found at the temperatures lower than approximately 2273 K [34]. The A-type hexagonal $Ce_2O_3$ will be not so stable at high temperature region. For $U = 0$, the curve is smooth. This should be due to the

inaccurate structural parameters produced by $U = 0$. By fitting the $B$–$T$ data from $U = 6$ eV to a third-order polynomial, we have the following relationship at 0 GPa:

$$B_0 = 138.83 - 2.09 \times 10^{-2}T - 1.64 \times 10^{-5}T^2 + 4.34 \times 10^{-9}T^3 \quad (8)$$

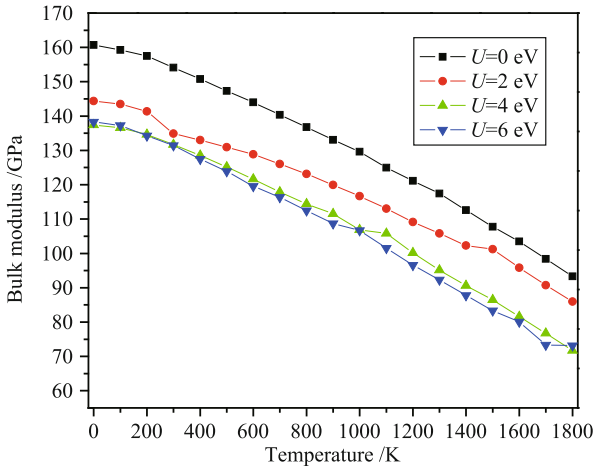


**Fig. 2** Bulk modulus versus temperature of $Ce_2O_3$ at 0 GPa when $U = 0$, 2, 4, and 6 eV, respectively.

The unit cell volumes at different temperatures with the increasing $U$ value can be directly derived from the quasi-harmonic Debye model, as are illustrated in Fig. 3. We can see that, at a given $U$ value, $V$ changes slightly with the increasing temperature when $T < 100$ K. Once $T > 100$ K, the volume will increase nearly linearly, showing great temperature effect. Just as we indicated in the previous discussion, the higher $U$ values have small effect on the $V$–$T$ curves, and the curves from different $U$ values will eventually merge with each other as the $U$ values increase. Especially, the obtained volume at 300 K (538 Bohr$^3$) agrees well with the experimental value (536 Bohr$^3$) when $U = 6$ eV.

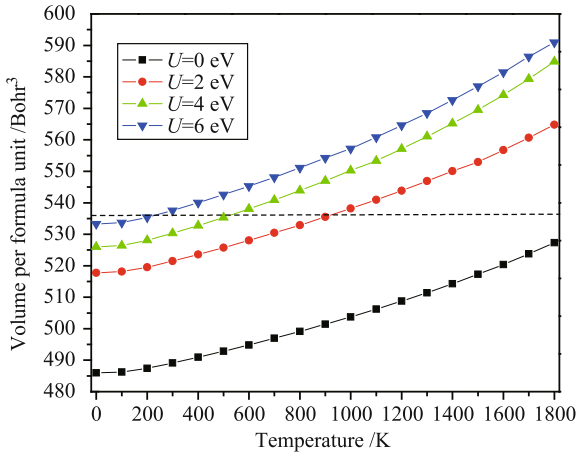


**Fig. 3** Primitive unit cell volume of $Ce_2O_3$ as a function of temperature with the applied $U$ values. The dot line represents the experimental value at the room temperature.

Thermal expansion parameters are important for predicting thermodynamic properties. Thus we obtain the variations of the thermal expansion coefficient $\alpha$ with temperature and different $U$ values in Fig. 4. It is seen that at a given $U$ value, $\alpha$ increases exponentially at low temperatures and approaches an approximately linear increase at high temperatures, which has a slightly upward trend after 1300 K. As the $U$ value increases, the increase of $\alpha$ with temperature becomes higher, especially at high temperature region. Nevertheless, the curves almost overlap with each other at high temperature region when $U = 4$ eV and 6 eV, which means that the temperature dependence of $\alpha$ suffers little impact from the higher $U$ values. It is important to notice that the neglect of intrinsic anharmonicity in the quasi-harmonic Debye model leads to an underestimation of thermal expansion at high temperatures in our calculations.

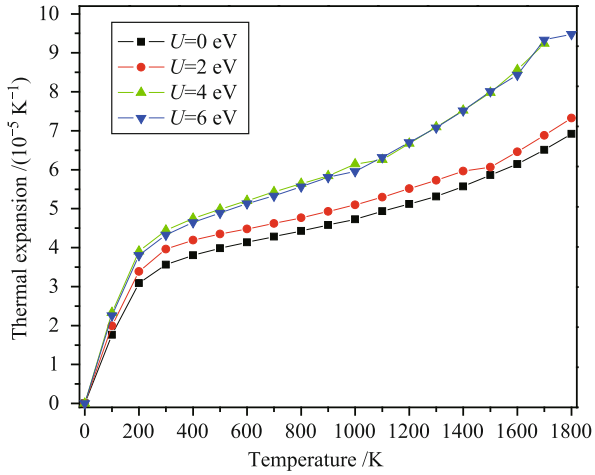


**Fig. 4** Temperature dependences of thermal expansion coefficient $\alpha$ of $Ce_2O_3$ at different $U$ values from LDA+$U$ method.

The Debye temperature is an important fundamental parameter and closely related to many physical properties of solids, such as the heat capacity and melting temperature. When below the Debye temperature, the quantum mechanical effects are very important in understanding the thermodynamic properties, while above the Debye temperature the quantum effects can be neglected. In Fig. 5, the variations of the Debye temperature $\Theta_D$ and the heat capacity $C_V$ are shown as a function of temperature at different $U$ values. The Debye temperature of $Ce_2O_3$ at 0 K and 0 GPa is 395.5 K. It is shown that, when the $U$ value keeps constant, the Debye temperature $\Theta_D$ decreases almost linearly within the applied temperatures, indicating the change of the vibration frequency of particles in $Ce_2O_3$ under different $U$ values. However,

in the same $U$ values, the heat capacity curve stays unchanged with the increasing $U$ value, indicating that the change of the $U$ value has no effect on the heat capacity $C_V$.

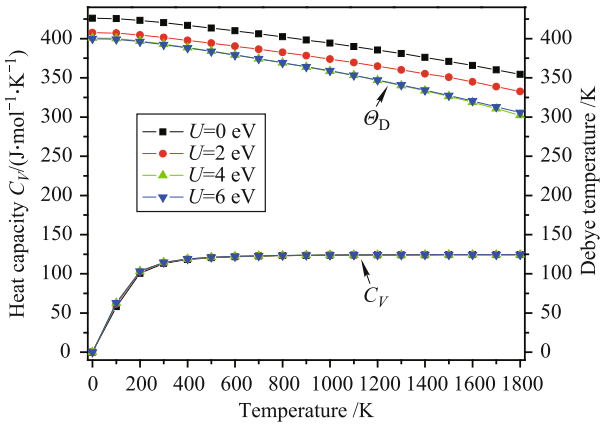


**Fig. 5** Temperature dependences of Debye temperature ($\Theta_D$) and heat capacity ($C_V$) of $Ce_2O_3$ at several $U$ values from LDA+$U$ method. The upper is the Debye temperature and the lower is the heat capacity.

Finally, the entropy $S$ and the heat capacities $C_P$ of $Ce_2O_3$ are plotted in Figs. 6 and 7 for several $U$ values, together with the experimental data [4, 5]. It is clear that the quasi-harmonic Debye model gives reasonable values for the entropy when compared with the experimental values [5]. Our calculated curve is close to the experimental curve with the increasing $U$ value. However, there is still existing a small deviation between the experimental data and our calculations at $U = 4$ eV and 6 eV. One reason is maybe that, our calculations are related to perfect crystal while the experimental samples include the defects. Another reason is that, the intrinsic anharmonicity is neglected in the quasi-harmonic approximation.

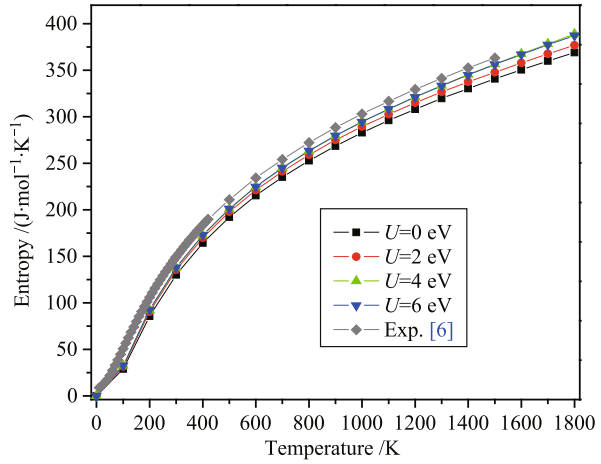


**Fig. 6** Calculated entropy by using LDA+$U$ method with different $U$ values and its comparison with experimental values. Note that in the experimental the values above $T = 900$ K are extrapolated.

From Fig. 7 it can be found that our calculations for the heat capacities $C_P$ up to the room temperature are consistent with the experimental value, while after the room temperature, the heat capacities $C_P$ is underestimated when $U$ equals 0 eV and 2 eV, and overestimated when $U$ equals 4 eV and 6 eV when compared to the experimental values [5]. These results indicate that the introduction of the $U$ value cannot only correct the calculation of the structure but also improve the accurate description of the thermodynamic properties of $Ce_2O_3$. It must be noted that in our calculations $Ce_2O_3$ is taken as anti-ferromagnet, but in fact the anti-ferromagnetism will disappear when the temperature above the Néel temperature.

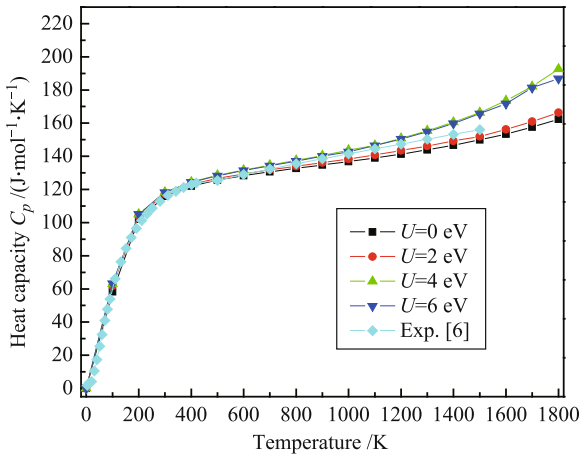


**Fig. 7** The heat capacity $C_p$ at different $U$ values and temperatures. Note that in the experiment the values above $T = 900$ K are extrapolated.

## 4 Conclusions

We have investigated the structural properties of $Ce_2O_3$ with different $U$ values by using local-density approximation (LDA) $+U$ correction scheme in the frame of density functional theory (DFT) with on-the-fly (OTF) pseudopotential. The lattice constants, bulk modulus and its pressure derivative $B_0'$, and the insulating gap obtained here are in good agreement with the available experimental data. Within the quasi-harmonic Debye model, the temperature dependences of the bulk modulus, thermal expansion coefficient, Debye temperature, specific heat as well as the entropy are discussed with the increasing $U$ value. It is found that the introduction of the $U$ value can improve the accurate description of the thermodynamic properties of $Ce_2O_3$. When $U = 6$ eV the obtained volume $V = 538$ Bohr$^3$ at 300 K agrees well with the experimental value (536 Bohr$^3$). The calculated entropy curves at $U = 4$ eV and 6 eV are closer to the

experimental curve than the curves from $U = 0$ eV and 2 eV. When $U$ equals 6 eV, there still exist small deviations between our calculations and experimental ones owing to the neglection of the intrinsic anharmonicity in the quasi-harmonic Debye model.

**Acknowledgements** The authors would like to thank the support by the National Natural Science Foundation of China (Grant Nos. 11204192 and 61176096). We also acknowledge the support for the computational resources by the State Key Laboratory of Polymer Materials Engineering of China in Sichuan University. Some calculations are performed on the ScGrid of Supercomputing Center, Computer Network Information Center of Chinese Academy of Sciences.



## References

1. A. Trovarelli, Catalysis by Ceria and Related Materials, London: Imperial College Press, 2002
2. M. Kobayashi and M. Ishii, Excellent radiation-resistivity of cerium-doped gadolinium silicate scintillators, *Nucl. Instrum. Methods B*, 1991, 61(4): 491
3. H. Kleykamp, The chemical state of the fission products in oxide fuels, *J. Nucl. Mater.*, 1985, 131(2–3): 221
4. B. H. Justice and E. F. Westrum, Thermophysical properties of the lanthanide oxides. V. Heat capacity, thermodynamic properties, and energy levels of cerium(III) oxide, *J. Phys. Chem.*, 1969, 73(6): 1959
5. M. E. Huntelaar, A. S. Booij, E. H. P. Cordfunke, R. R. van der Laan, A. C. G. van Genderen, and J. C. van Miltenburg, The thermodynamic properties of $Ce_2O_3$ (s) from $T \rightarrow 0$ K to 1500 K, *J. Chem. Thermodyn.*, 2000, 32(4): 465
6. N. V. Skorodumova, R. Ahuja, S. I. Simak, I. A. Abrikosov, B. Johansson, and B. I. Lundqvist, Electronic, bonding, and optical properties of $CeO_2$ and $Ce_2O_3$ from first principles, *Phys. Rev. B*, 2001, 64(11): 115108
7. A. J. Cohen, P. Mori-sanchez, and W. T. Yang, Insights into current limitations of density functional theory, *Science*, 2008, 321(5890): 792
8. H. Jiang, R. I. Gomez-Abal, P. Rinke, and M. Scheffler, Localized and itinerant states in lanthanide oxides united by GW@LDA+$U$, *Phys. Rev. Lett.*, 2009, 102(12): 126403
9. N. V. Skorodumova, S. I. Simak, B. I. Lundqvist, I. A. Abrikosov, and B. Johansson, Quantum origin of the oxygen storage capability of ceria, *Phys. Rev. Lett.*, 2002, 89(16): 166601
10. C. Loschen, J. Carrasco, K. M. Neyman, and F. Illas, First-principles LDA+$U$ and GGA+$U$ study of cerium oxides: Dependence on the effective $U$ parameter, *Phys. Rev. B*, 2007, 75(3): 035115
11. D. A. Andersson, S. I. Simak, B. Johansson, I. A. Abrikosov, and N. V. Skorodumova, Modeling of $CeO_2$, $Ce_2O_3$, and $CeO_{2-x}$ in the LDA+$U$ formalism, *Phys. Rev. B*, 2007, 75(3): 035109
12. J. Graciani, A. M. Márquez, J. J. Plata, Y. Ortega, N. C. Hernández, A. Meyer, C. M. Zicovich-Wilson, and J. F. Sanz, Comparative study of the performance of hybrid DFT functionals in highly correlated oxides: The case of $CeO_2$ and $Ce_2O_3$, *J. Chem. Theory Comput.*, 2011, 7(1): 56
13. Y. Y. Qi, Z. W. Niu, C. Cheng, and Y. Cheng, Structural and elastic properties of $Ce_2O_3$ under pressure from LDA+$U$ method, *Front. Phys.*, 2013, 8(4): 405
14. M. C. Payne, M. P. Teter, D. C. Allen, T. A. Arias, and J. D. Joannopoulos, Iterative minimization techniques for ab initio total-energy calculations: Molecular dynamics and conjugate gradients, *Rev. Mod. Phys.*, 1992, 64(4): 1045
15. V. Milman, B. Winkler, J. A. White, C. J. Packard, M. C. Payne, E. V. Akhmatskaya, and R. H. Nobes, Electronic structure, properties, and phase stability of inorganic crystals: A pseudopotential plane-wave study, *Int. J. Quantum Chem.*, 2000, 77(5): 895
16. A. Otero-de-la-Roza and V. Luaña, Gibbs2: A new version of the quasi-harmonic model code. I. Robust treatment of the static data, *Comput. Phys. Commun.*, 2011, 182(8): 1708
17. A. Otero-de-la-Roza, D. Abbasi-Pérez, and V. Luaña, GIBBS2: A new version of the quasiharmonic model code. II. Models for solid-state thermodynamics, features and implementation, *Comput. Phys. Commun.*, 2011, 182(10): 2232
18. S. H. Vosko, L. Wilk, and M. Nusair, Accurate spin-dependent electron liquid correlation energies for local spin density calculations: A critical analysis, *Can. J. Phys.*, 1980, 58(8): 1200
19. V. I. Anisimov, I. V. Solovyev, and M. A. Korotin, Density-functional theory and NiO photoemission spectra, *Phys. Rev. B*, 1993, 48(23): 16929
20. M. Cococcioni and S. de Gironcoli, Linear response approach to the calculation of the effective interaction parameters in the LDA+$U$ method, *Phys. Rev. B*, 2005, 71(3): 035105
21. H. J. Monkhorst and J. D. Pack, Special points for Brillouin-zone integrations, *Phys. Rev. B*, 1976, 13(12): 5188
22. L. Y. Lu, X. R. Chen, B. R. Yu, and Q. Q. Gou, First-principles calculations for transition phase and thermodynamic properties of GaAs, *Chin. Phys.*, 2006, 15(4): 802
23. X. L. Zhou, K. Liu, X. R. Chen, and J. Zhu, Structural and thermodynamic properties of $AlB_2$ compound, *Chin. Phys.*, 2006, 15(12): 3014
24. Y. J. Hao, Y. Cheng, Y. J. Wang, and X. R. Chen, Elastic and thermodynamic properties of c-BN from first-principles calculations, *Chin. Phys.*, 2007, 16(1): 217
25. J. Chang, X. R. Chen, W. Zhang, and J. Zhu, First-principles investigations on elastic and thermodynamic properties of zinc-blende structure BeS, *Chin. Phys. B*, 2008, 17(4): 1377
26. X. F. Li, G. F. Ji, F. Zhao, X. R. Chen, and D. Alfe, First-principles calculations of elastic and electronic properties of $NbB_2$ under pressure, *J. Phys.: Condens. Matter*, 2009, 21(2): 025505

27. H. Z. Guo, X. R. Chen, L. C. Cai, and J. Gao, Structural and thermodynamic properties of $MgB_2$ from first-principles calculations, *Solid State Commun.*, 2005, 134(3): 787

28. X. L. Yuan, D. Q. Wei, Y. Cheng, G. F. Ji, Q. M. Zhang, and Z. Z. Gong, Pressure effects on elastic and thermodynamic properties of $Zr_3Al$ intermetallic compound, *Comp. Mater. Sci.*, 2012, 58(2) : 125

29. H. Barnighausen and G. Schiller, The crystal structure of alfa-$Ce_2O_3$, *J. Less-Common Met.*, 1985, 110(1–2): 385

30. P. J. Hay, R. L. Martin, J. Uddin, and G. E. Scuseria, Theoretical study of $CeO_2$ and $Ce_2O_3$ using a screened hybrid density functional,*J. Chem. Phys.*, 2006, 125(3): 034712

31. J. Heyd and G. E. Scuseria, Assessment and validation of a screened Coulomb hybrid density functional, *J. Chem. Phys.*, 2004, 120(16): 7274

32. F. Birch, Finite elastic strain of cubic crystals, *Phys. Rev.*, 1947, 71(11): 809

33. A. V. Prokofiev, A. I. Shelykh, and B. T. Melekh, Periodicity in the band gap variation of $Ln_2X_3$ (X = O, S, Se) in the lanthanide series, *J. Alloy. Comp.*, 1996, 242(1–2): 41

34. G. Y. Adachi and N. Imanaka, The binary rare earth oxides, *Chem. Rev.*, 1998, 98: 1479